SIMULATION OF THE RF COUPLER FOR TRIUMF ISAC-II SUPERCONDUCTING QUARTER WAVE RESONATORS

V. Zvyagintsev, TRIUMF*, 4004 Wesbrook Mall, Vancouver, Canada, V6T2A3

Abstract

The inductive RF coupler for the TRIUMF ISAC-II 106 MHz superconducting accelerating quarter wave resonators [1, 2] was used as a basis for the simulation model of stationary transmission processes of RF power and thermal fluxes. Electromagnetic simulation of the coupler was done with ANSOFT HFSS code. Transmission line theory [3] was used for electromagnetic wave calculations along the drive line to the Coupler. An analogy between electric and thermal processes allows the thermal calculations to be expressed in terms of electrical circuits [4]. The data obtained from the simulation are compared to measured values on the RF coupler.

INTRODUCTION

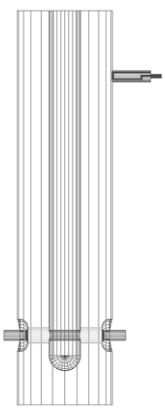

fo	MHz	106
E_a	MV/m	6
P	W	4
Q_o		5.5E+08
U	J	3.3
B_p	mT	60
Δf	Hz	40
β		200
P_f	W	200

$$1/Q_L = 1/Q_o + 1/Q_e \qquad \beta = Q_o/Q_e$$

$$P_f = P\frac{(\beta+1)^2}{4\beta} \qquad \Delta f_L = f_o/Q_L$$

Figure 1: HFSS model of SC TRIUMF ISAC-II medium-β QWR with inductive coupler.

The inductive coupler for the TRIUMF ISAC-II 106 MHz superconducting accelerating quarter wave resonators was designed and successfully tested. The main goal of the design is achieved: the coupler provides more than 200 W forward power which is needed to get an accelerating field E_a=6 MV/m with a bandwidth 40 Hz to maintain a stable cavity operation disturbed by noise and helium pressure fluctuations and thermal load for helium system from the coupler is less than 1 W. Coupler R&D was done with test cryostat and the first TRIUMF ISAC-II cryomodule with 4 medium-β cavities was equipped with new couplers and succesefully tested [1].

* TRIUMF receives funding via a contribution agreement through the National Research Council of Canada

This paper is some attempt to collect the calculation experience from this R&D which can be used for coupler design for next TRIUMF ISAC-II cryomodules which will be equipped with high-β resonators.

HFSS COUPLER SIMULATION

Coupling and Loop Power Dissipation

Due to very high Q of the cavity it is not possible to use the driven mode solution so the eigenmode solution was used instead. For simulation purposes it was assumed that the cavity and coupler were perfect conductors. The coupler port is loaded with an equivalent impedance of 50 Ω. The mesh is refined in the beam and coupler region. The power dissipation on the loop was calculated in the Postprocessor by using normalization for acceleration

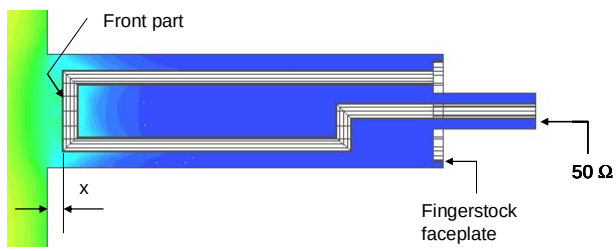

Figure 2: Magnetic field and port bondary condition for HFSS coupling loop model.

field E_a=6 MV/m and conductivity of copper. P_{loop} is the total power dissipated on the loop and P_{front} is the power dissipated on the front part of the loop which is used for analytical check. Data obtained in HFSS calculations at different loop positions are shown in Table 1. Power dissipated on the loop is due to field penetration from the cavity and rf current to the 50 Ω load. In the driven mode which is the real condition for overcoupled operation, the rf current will be very small because a current node appears at the loop as shown in Fig.7. Power dissipation in the load is inversely proportional to the quality factor. By using the external quality factor Q from table 1, and power dissipation P and quality factor Q_o from Fig.1, then power dissipation in the load and power dissipation on the loop due to the rf current through the load P_{loop}* can be calculated (to make a coorection for driven mode). Power dissipation on the loop P_{loop}** for strong overcoupled driven mode is a difference between power dissipation for eigen mode P_{loop} and P_{loop}*. The external quality factor can be defined from the following expression:

$$1/Q_e = 1/Q + 1/Q_{loop} \qquad (1)$$

Loop quality factor defined from loop power dissipation

$$Q_{loop} = 2\pi f_o \frac{U}{P_{loop}} \quad (2)$$

Coupling, bandwidth and forward power (Table 2) are defined according to the well known expressions which are shown in Fig. 1.
Fig.3 is a graph which was created from Table 2 and may be used to define the operating parameters of the

Table 1: HFSS eigensolver calculations of coupling and loop power dissipation for E_a=6 MV/m, f_o=105.940 MHz

x	Q	P_{loop}	P_{front}	P_{loop}*
mm		W	W	W
0	1.37E+06	15.7	10.6	1.495
3	3.49E+06	7.64	4.82	0.585
6	9.35E+06	2.69	1.72	0.219
9	2.50E+07	1.06	0.67	0.082
12	6.75E+07	0.38	0.25	0.030
15	1.85E+08	0.15	0.10	0.011
18	5.12E+08	0.06	0.04	0.004
21	1.48E+09	0.02	0.01	0.001

Table 2: Interpretation of eigensolver HFSS calculations for coupling parameters of the QWR at E_a=6 MV/m

x	Q_L	β	Δf	P_f
mm			Hz	W
0	1.35E+06	410	78.5	412
3	3.43E+06	161	30.9	163
6	9.10E+06	60.0	11.7	62.1
9	2.36E+07	22.5	4.49	24.5
12	5.96E+07	8.31	1.78	10.4
15	1.38E+08	3.04	0.77	5.37
18	2.65E+08	1.10	0.40	4.01
21	4.02E+08	0.38	0.26	5.00

cavity for the ISAC II operation at Ea=6 MV/m. For example, for a bandwidth of 40 Hz the loop position is 2.5 mm, the forward power is 200 watts and the power on the loop is is ~8 watts. After correction by Ploop* value which is ~1 W, power dissipation on the loop becomes ~7 W.

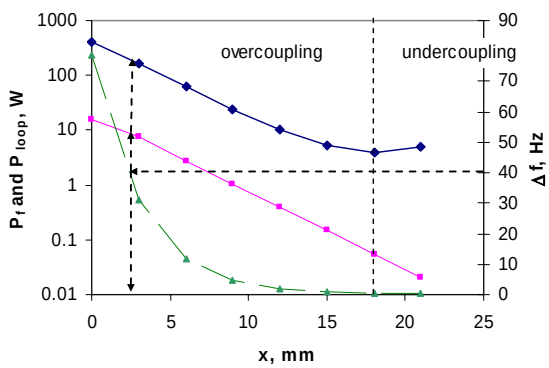

Figure 3: Operating rf parameters of the coupled QWR.

This value should be considered in the thermal design as a potential thermal load for the helium system. During the TRIUMF coupler test we observed effects of loop heating producing a change in the coupling.

Analytical Check

Power dissipation on the front part of the loop (P_{front}) was checked analytically by considering the penetration of the field from the cavity to the coupler housing for the lowest H_{11} mode. The critical wavelength [4] for the coupler housing cylinder with a radius 11 mm is 38 mm and the constant of penetration is γ=167. The field attenuation for loop position of 21 mm is

$$A_{dB} = 20\lg(e^{-\gamma x}) \approx 30dB \quad (3)$$

which is consistent with the P_{front} variation for x values from 0 to 21 mm in Table 1.
Considering the QWR as a lossless transmission line with longitudinal cosine field distribution and using Ampere's law, the magnetic field on the front part of the loop at x=0 is given by:

$$H_{loop} = H_p \frac{r}{R}\cos\left(\frac{2\pi}{\lambda} l_c\right) \quad (4)$$

where r and R are inner and outer radius of the QWR, lc is the distance from the shorted flange of the QWR to the coupler loop. Power dissipation on the front part of the loop is given by:

$$P^*_{front} = \frac{R_s}{2}\int_S |j|^2 ds \approx \frac{R_s}{2}\cdot S \cdot H_{loop}{}^2 \approx 15W \quad (5)$$

By using formula (3) for field attenuation and 15 W for P_{front} at x=0 we can calculate this power for different loop positions. Fig. 4 shows the comparison of numerical and analytical results for power dissipation on the front part of the loop Pfront. Numerical and analytical results are consistent.

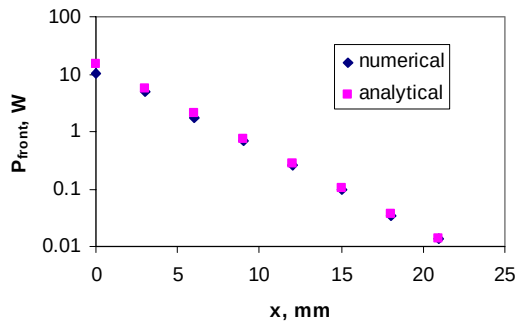

Figure 4: Numerical and analytical Pfront comparison at E_a=6 MV/m.

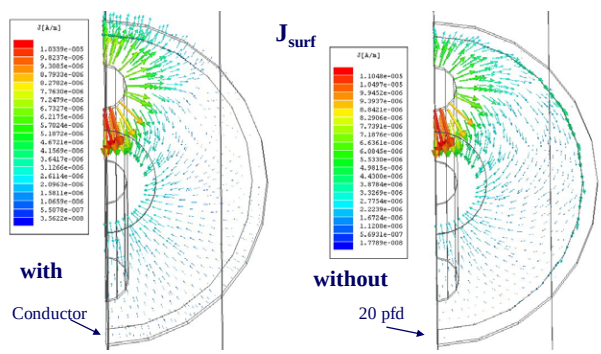

Figure 5: Rf current density distribution on the faceplate of the coupler with and without fingerstock

Fingerstock Problem

Rf fingerstock was initially installed in the coupling loop assembly to provided an rf path to ground for any rf leakage from the cavity through the coupling loop penetration. However this also caused micro dust in the coupling loop housing. To simulate the coupler without fingerstock the boundary condition on the figerstock faceplate (Fig. 2) was changed from a perfect conductor to a capacitive impedance which is eqiuvalent to minimum capacitance of 20 pfd between the coupler body and the coupler housing. This calculation was done for x=3 mm which is close to the operation condition of the cavity. Without fingerstock the same values of resonant frequency and quality factor were obtained. This means that removing the fingerstock does not cause coupling degradation. A coupler test without the fingerstock showed the same coupler performance but more rf leakadge was observed indicated by increased noise on some temperature sensors.

Without the fingerstock the current is no longer perpendicular to the faceplate edge which implies more rf radiation as can be seen in Fig. 5.

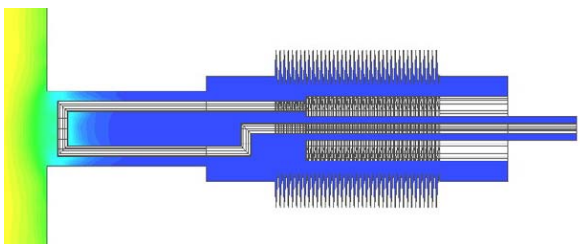

Figure 6: Magnetic field in the HFSS model of coupler with bellows.

Another option to avoid rf leakage is a coupler with bellows which could be used for a separate vacuum design. A HFSS model simulation (Fig. 6) showed a good performance and very low rf losses on the bellows.

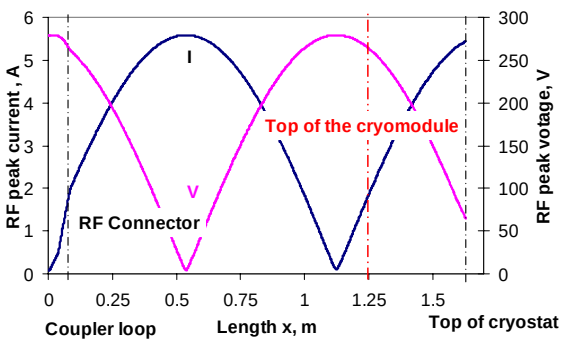

Figure 7: The voltage and current distribution along the coupling line inside of the test cryostat at nominal operating parameters (E_a=6 MV/m, P_f=200 W).

Coupler Drive Line

The most critical part of the coupler drive line is inside of the cryostat. The voltage and current distribution along the line (Fig. 7) are calculated by using well known transmission line theory [3] and considering the line as a chain of elements from the coupling loop (which is a load) to the rf feedthrough on the top of the cryostat (which is the input). Power dissipation on the line at such frequency arises mainly from Joule heating and it is very important to keep rf connectors away from maximum current regions. One can see from Fig. 7 that the length of the coupler line inside of the cryostat is unfortunate and puts the rf feedthrough at a current maximum which caused heating problems. However for the cryomodule the connector is closer to the current minimum and caused no trouble during the test [1].

Thermal Calculations

Thermal calculations were conducted by using an analogy of electrical and thermal processes [4]. Fig.8 shows an example of cell element schematic for thermal analysis which presents power dissipation as current sources and resistors represent properties of the elements for longitudinal and transverse thermal conductivity and heat radiation. The temperature of heat sinks is presented as potentials. The model can be

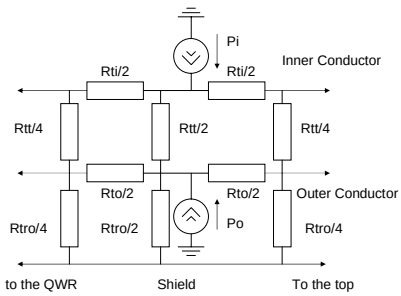

Figure 8: Example of electro-thermical equivalent cell.

solved with standard schematic solvers like PSpice. This technique can be used just for comparison of design options because it is very difficult to predict real cryogenics thermal parameters of contacts.

CONCLUSIONS

The goal for the coupler design is to provide a good rf performance at minimum heat load for helium cryogenics system. HFSS simulation of coupler and coupler line calculations provide some values of thermal loads which should be considered in thermal considerations and calculations to estimate ways to maintain good cryogenic performance of the coupler system.

REFERENCES

[1] R. Poirier, et al, RF coupler design for the TRIUMF ISAC-II superconducting quarter wave resonator, LINAC 2004, MOP88.

[2] A. Facco, et al, Superconducting medium beta prototype for radioactive beam acceleration at TRIUMF, PAC 2001, MPPH134.

[3] J. Dunlop, D. G. Smith. Telecommunications Engineering, 3rd edition 1994.

[4] DOE Fundamentals Handbook. Thermodynamics, heat transfer and fluid flow. Volume 2 of 3.